THE ASTROPHYSICAL JOURNAL, Vol. 153, July 1968

RESONANT PERIODIC ORBITS

G. CONTOPOULOS
Goddard Institute for Space Studies, NASA, New York, and
Thessaloniki University, Thessaloniki, Greece
Received November 27, 1967

ABSTRACT

Resonant periodic orbits, making n oscillations along the x-axis and m oscillations along the y-axis, appear in a two-dimensional potential $V = \frac{1}{2}(Ax^2 + By^2)$ + higher-order terms whenever the ratio $A^{1/2}/B^{1/2}$ is near n/m. Such orbits can be found by means of a "third" integral in which small divisor terms have been eliminated. Orbits whose initial conditions are near those of a stable resonant periodic orbit are tube orbits. By finding the main periodic orbits, one can derive the main characteristics of the totality of orbits. An application in the case $A^{1/2}/B^{1/2} \simeq \frac{2}{3}$ is given. These considerations can be applied to find the main types of orbits in various galactic models.

I. INTRODUCTION

In a previous paper (Contopoulos 1965) we explained the formation of resonant periodic orbits and tube orbits in the case of a potential of the general form $V = \frac{1}{2}(Ax^2 + By^2)$ + higher-order terms. The resonant periodic orbits make n oscillations along the x-axis and m oscillations along the y-axis whenever the ratio of unperturbed frequencies $A^{1/2}/B^{1/2}$ is near n/m; the tube orbits always stay near the stable resonant periodic orbits.

In the above paper we found the properties of the resonant periodic orbits and the tube orbits by means of the third integral. The method was based on the elimination of the secular terms of the third integral in the resonance case $A^{1/2}/B^{1/2} = n/m$. By using the new form of the third integral, we could find the forms of the invariant curves on a surface of section. Of special interest are the invariant points corresponding to resonant periodic orbits; the stable resonant invariant points are surrounded by islands, corresponding to tube orbits.

This method has been extended to near-resonance cases. In these cases, instead of secular terms we have terms with small divisors, which may become very large.

In general, we may consider that a given ratio of unperturbed frequencies $A^{1/2}/B^{1/2}$ is "near" many rational values n/m. If the difference $|(A^{1/2}/B^{1/2}) - (n/m)|$ is smaller than a certain quantity e, then resonant periodic orbits making n and m oscillations along the x- and y-axes, respectively, appear, followed by the tube orbits. If the potential is of the form $V = \frac{1}{2}(Ax^2 + By^2) - \epsilon xy^2$, the quantity e is of order $\epsilon^2 h$, where h is the energy (Contopoulos 1966).

For any value of $A^{1/2}/B^{1/2}$ we have an infinity of periodic and tube orbits of different types. However, the most important of them correspond to small values of n and m.

In order to find theoretically the periodic orbits and the tube orbits of a certain type, we have to eliminate the corresponding small divisor terms of the third integral. This can be done by means of a computer program similar to the one used previously to give tables of the coefficients of the third integral (Contopoulos 1966). The present method takes care of the cases where these coefficients are infinite or large.

II. ELIMINATION OF SMALL DIVISORS

We consider, as an example, the potential

$$V = \frac{1}{2}(Ax^2 + By^2) - \epsilon xy^2 . \tag{1}$$

The third integral is constructed in the usual way (Contopoulos 1960)

$$\Phi_1 = \Phi_{10} + \epsilon\Phi_1 + \ldots , \tag{2}$$

where

$$\Phi_{10} = \tfrac{1}{2}(Ax^2 + X^2) \tag{3}$$

contains terms with small divisors of the form $mA^{1/2} - nB^{1/2}$ in $\Phi_{1,m+n-2}$.

In fact, we have

$$\Phi_{1,m+n-2} = -\int (\Phi_{1,m+n-3},\ H_1)dt , \tag{4}$$

where

$$H_1 = -xy^2 , \tag{5}$$

and $(\Phi_{1,m+n-3}, H_1)$ is the Poisson bracket. This Poisson bracket is a polynomial of degree $m + n$ in x, X, y, Y, and it can be easily expressed as a sum of trigonometric terms of the form

$$q(2\Phi_{10})^{m_1/2}(2\Phi_{20})^{n_1/2} \begin{matrix}\sin\\ \cos\end{matrix} [m_1 A^{1/2}(t - t_0) - n_1 B^{1/2}t] ,$$

if the variables are replaced by the solutions of the unperturbed problem

$$\begin{aligned} x &= \frac{(2\Phi_{10})^{1/2}}{A^{1/2}} \sin A^{1/2}(t - t_0) , \quad & y &= \frac{(2\Phi_{20})^{1/2}}{B^{1/2}} \sin B^{1/2}t , \\ X &= (2\Phi_{10})^{1/2} \cos A^{1/2}(t - t_0) , \quad & Y &= (2\Phi_{20})^{1/2} \cos B^{1/2}t , \end{aligned} \tag{6}$$

where

$$\Phi_{20} = \tfrac{1}{2}(By^2 + Y^2) , \tag{7}$$

m_1 and n_1 are integers, and n_1 is always even. Among these terms, one can separate the terms of the form

$$q(2\Phi_{10})^{m/2}(2\Phi_{20})^{n/2} \begin{matrix}\cos\\ \sin\end{matrix} [mA^{1/2}(t - t_0) - nB^{1/2}t] ,$$

which give rise to small divisor terms after integration. We have the cosine if $m + n$ is odd and the sine if $m + n$ is even.

This procedure can be easily carried out by a computer program, which gives directly the coefficient q. This program is a slight modification of a program used to calculate the terms of the third integral (Contopoulos 1966).

The elimination of the secular terms is effected as follows: By multiplying the integral (2) by $(mA^{1/2} - nB^{1/2})$, we find the integral

$$\phi_1 = \Phi_1(mA^{1/2} - nB^{1/2}) , \tag{8}$$

which does not contain small divisor terms of degree $m + n$. However, small divisors appear in the term $\Phi_{1,m+n}(mA^{1/2} - nB^{1/2})$, of degree $m + n + 2$, which are of the form

$$[q_1(2\Phi_{10}) + q_2(2\Phi_{20})]Q , \tag{9}$$

where

$$Q = \frac{(2\Phi_{10})^{m/2}(2\Phi_{20})^{n/2}}{mA^{1/2} - nB^{1/2}} \begin{matrix}\sin\\ \cos\end{matrix} [mA^{1/2}(t - t_0) - nB^{1/2}t] . \tag{10}$$

Here we always have the sine if $m + n$ is odd and the cosine if $m + n$ is even. At the same time, one can construct equivalent forms of the third integral, beginning with $(2\Phi_{10})^2$ or $(2\Phi_{20})^2$, namely,

$$\phi_2 = (2\Phi_{10})^2 + \epsilon\phi_{21} + \ldots \quad \text{and} \quad \phi_3 = (2\Phi_{20})^2 + \epsilon\phi_{31} + \ldots . \tag{11}$$

These expansions give terms with small divisors, of degree $m + n + 2$, of the form $(2\Phi_{10})q_1'Q$ and $(2\Phi_{20})q_2'Q$, respectively.

Then the integral

$$\phi = c(\phi_1 + c_1\phi_2 + c_3\phi_3) \tag{12}$$

has no small divisor terms of degree $m + n + 2$ if

$$q_1 + c_1 q_1' = 0 , \quad q_2 + c_2 q_2' = 0 , \tag{13}$$

and c is any arbitrary constant. The values of q_1, q_2, q_1', q_2' are given by the computer, hence c_1, c_2 are easily calculated. To this integral we may add any multiple of

$$\phi_4 = (2H)^2 = (2\Phi_1 + 2\Phi_2)^2 = (2\Phi_{10} + 2\Phi_{20})^2 + \epsilon\phi_{41} + \ldots , \tag{14}$$

where H is the Hamiltonian; this integral does not give small divisor terms at all.

In order to avoid now the small divisor terms of degree $m + n + 4$, we find the terms with small divisors of degree $m + n + 4$ in the expansions

$$\begin{aligned} \bar{\phi}_1 &= \phi_1 + c_1\phi_2 + c_3\phi_3 , & \bar{\phi}_2 &= (2\Phi_{10})^3 + \epsilon\bar{\phi}_{21} + \ldots , \\ \bar{\phi}_3 &= (2\Phi_{10})^2(2\Phi_{20}) + \epsilon\bar{\phi}_{31} + \ldots , \quad \text{and} & \bar{\phi}_4 &= (2\Phi_{20})^3 + \epsilon\bar{\phi}_{41} + \ldots , \end{aligned} \tag{15}$$

which are

$$\begin{gathered} [\bar{q}_1(2\Phi_{10})^2 + \bar{q}_2(2\Phi_{10})(2\Phi_{20}) + \bar{q}_3(2\Phi_{20})^2]Q , \\ [\bar{q}_1'(2\Phi_{10})^2 + \bar{q}_2'(2\Phi_{10})(2\Phi_{20}) + \bar{q}_3'(2\Phi_{20})^2]Q , \\ [\bar{q}_1''(2\Phi_{10})^2 + \bar{q}_2''(2\Phi_{20})(2\Phi_{20}) + \bar{q}_3''(2\Phi_{20})^2]Q , \quad \text{and} \quad \bar{q}_3'''(2\Phi_{20})^2Q , \end{gathered} \tag{16}$$

respectively. No small divisor terms of smaller degree appear. Now we determine the constants d_1, d_2, d_3 so that the integral

$$\phi = c(\bar{\phi}_1 + d_1\bar{\phi}_2 + d_3\bar{\phi}_3 + d_4\bar{\phi}_4) \tag{17}$$

does not contain terms with small divisors up to the degree $m + n + 4$. We have the following equations:

$$\begin{gathered} \bar{q}_1 + d_1\bar{q}_1' + d_3\bar{q}_1'' = 0 , \quad \bar{q}_2 + d_1\bar{q}_2' + d_3\bar{q}_2'' = 0 , \\ \bar{q}_3 + d_1\bar{q}_3' + d_3\bar{q}_3'' + d_4\bar{q}_3''' = 0 , \end{gathered} \tag{18}$$

which give the values of d_1, d_2, d_3. In the same way we can avoid terms with small divisors of higher degrees.

In the case $m = 2$, $n = 3$ we have calculated c_1, c_2, d_1, d_2, d_3 for various values of the ratio $A^{1/2}/B^{1/2}$. In order to check the computer calculations, we have calculated analytically the values of c_1, c_2 in the case $m = 2$, $n = 3$, $A = 0.391$, $B = 0.9$.

The new form of the third integral ϕ is now used in finding the resonant periodic orbits and their stability.

III. DETERMINATION OF PERIODIC ORBITS AND THEIR STABILITY

The successive points of intersection of an orbit by a surface of section are, in general, on a smooth invariant curve. This is true for most initial conditions (except for a set of very small measure if the perturbation ϵ is sufficiently small; such is the case that we consider below). We take as surface of section the plane $y = 0$ in the space $\bar{x}yX$, where $\bar{x} = A^{1/2}x$.

Of special interest are the invariant points, which correspond to periodic orbits. Besides a "central" invariant point, corresponding to a stable periodic orbit perpendicular to the x-axis at one point near the origin, there are other "resonant" invariant points, corresponding to orbits making n and m oscillations along the x-axis and the y-axis, respectively. These are stable or unstable. In the first case, nearby orbits are tube orbits and the corresponding invariant curves are called islands, surrounding the stable invariant points.

In order to find experimentally the resonant periodic orbits, a computer program was developed to give periodic orbits of the above resonance form to any required accuracy. This program calculates orbits intersecting perpendicularly the x-axis for a given value of the energy h. The initial conditions are x_0, $y_0 = X_0 = 0$, $Y_0 = (2h - Ax_0^2)^{1/2}$, where x_0 takes successive values in the interval $-(2h/A)^{1/2}$, $(2h/A)^{1/2}$, differing by a fixed step. The calculation stops when y becomes zero for the $(2m)$th time. (An interpolation formula gives the value of X when y approaches zero, to any required accuracy.) Then if two successive final values of X have opposite signs, by successive interpolations we find the initial value of x_0, corresponding to the periodic orbit ($X = 0$), with any required accuracy.

On the other hand, a theoretical search of periodic orbits was made by means of the third integral, after elimination of the small divisors. A careful elimination of the small divisors has proved necessary because otherwise higher-order terms of the third integral may change considerably the results found by using only the first few terms.

Let

$$\phi = \phi_{;0} \tag{19}$$

be the series representing the third integral after elimination of the small divisors; the zero after the semicolon means that the function is evaluated at the initial point.

We set $y = 0$ and use the energy integral

$$Y^2 = 2h - Ax^2 - X^2 , \tag{20}$$

where h is the total energy, to make ϕ a function of x and X only. From our first paper on the third integral (Contopoulos 1960) we can see that any term $x^a X^b y^c Y^d$ has $c + d =$ even and $b + d =$ even. Hence if $y = 0$, the terms that remain in ϕ have Y and X in even powers

It is preferable, for some purposes, to use $\bar{x} = A^{1/2}x$, instead of x. Thus ϕ is a function of $\bar{x}$ and X^2 only, and we can write

$$\phi = \bar{\phi} + X^2\phi_X , \tag{21}$$

where $\bar{\phi}$ contains only $\bar{x}$, while ϕ_X contains $\bar{x}$ and X^2.

A closed invariant curve issuing from a point $\bar{x}_0$, $X_0 = 0$ on the $\bar{x}$-axis intersects the $\bar{x}$-axis at the points given by the equation

$$\bar{\phi} = \bar{\phi}_{;0} . \tag{22}$$

This equation gives, in general, one more solution besides $\bar{x}_0$. If, however, $\bar{x}_0$ happens to correspond to a periodic orbit, the two solutions coincide and $\bar{x}_0$ is a double root of equation (22). Thus the invariant points are given by the solutions of the equation

$$d\bar{\phi}/d\bar{x} = 0 . \tag{23}$$

These are singular points of the curve $\phi = \phi_{;0}$ because then

$$\partial\phi/\partial\bar{x} = \partial\phi/\partial X = 0 . \tag{24}$$

In practice, the computer solves equation (23) if ϕ is already known in a truncated form. In fact, the computer selects only terms independent of X and y, which are of the form

$$\bar{\phi} = \Sigma C \bar{x}^a Y^d = \Sigma C \bar{x}^a (2h - \bar{x}^2)^{d/2} , \tag{25}$$

where d is even. The derivative of $\bar{\phi}$ is then

$$\frac{d\bar{\phi}}{d\bar{x}} = \sum C[a\bar{x}^{a-1}(2h - \bar{x}^2)^{d/2} - d\bar{x}^{a+1}(2h - \bar{x}^2)^{d/2-1}] . \tag{26}$$

The stability of the periodic orbits can be studied as follows. A singular point of the curve $\phi = \phi_{;0}$ is either isolated or a double point. In the first case, the equation

$$\frac{\partial^2 \phi}{\partial \bar{x}^2} \Delta\bar{x}^2 + 2 \frac{\partial^2 \phi}{\partial \bar{x} \partial X} \Delta\bar{x}\Delta X + \frac{\partial^2 \phi}{\partial X^2} \Delta X^2 = 0 \tag{27}$$

has no real roots for $\Delta\bar{x}/\Delta X$, while, in the second case, it has two real roots, in general. If $X = 0$, we have $\partial^2\phi/\partial\bar{x}\partial X = 0$; hence the discriminant of the above equation is

$$- 4 \frac{\partial^2 \phi}{\partial \bar{x}^2} \frac{\partial^2 \phi}{\partial X^2} .$$

Further, for $X = 0$ we have

$$\frac{\partial^2 \phi}{\partial \bar{x}^2} = \frac{\partial^2 \bar{\phi}}{\partial \bar{x}^2} , \tag{28}$$

and

$$\frac{\partial^2 \phi}{\partial X^2} = 2\phi_X(X = 0) . \tag{29}$$

Hence, finally, we have stability if the discriminant is negative, or

$$\frac{\partial^2 \bar{\phi}}{\partial \bar{x}^2} \phi_X \, (X = 0) > 0 , \tag{30}$$

and instability if the discriminant is positive, or

$$\frac{\partial^2 \bar{\phi}}{\partial \bar{x}^2} \phi_X \, (X = 0) < 0 . \tag{31}$$

The above analysis refers to cases when the periodic orbit intersects the x-axis perpendicularly ($X = 0$). But it may be that the invariant points corresponding to a periodic orbit are all outside the x-axis. Then in general there is another periodic orbit that has two invariant points on the x-axis (Contopoulos 1965). By finding this second periodic orbit, one can find the approximate position of the invariant points of the first orbit. A better estimate of their position is found by calculating the islands corresponding to a nearby tube orbit.

One should remark that the above method does not give all the periodic orbits in a given potential and a given value of the energy. In order to find resonant periodic orbits corresponding to a different commensurability (i.e., corresponding to another ratio n'/m', which is also near $A^{1/2}/B^{1/2}$), one has to find another form of the third integral, by eliminating the small divisors $m'A^{1/2} - n'B^{1/2}$. If the perturbation ϵ is not very large, the various kinds of periodic orbits are completely independent. The corresponding invariant points and islands are well separated.

This means that the form of the third integral is not unique for a given value of the energy integral. In some part of the surface of section, a given expression $\phi = \phi_{;0}$ gives the positions of the invariant points and the forms of the islands. In other parts, another form of the third integral is necessary. In fact, an infinity of forms is needed to explain all the periodic orbits. If, however, we are interested only in the main invariant points and islands, then one or two forms of the third integral may be sufficient.

IV. APPLICATION

We apply the above method in the case $A^{1/2}/B^{1/2} \simeq \frac{2}{3}$. In this special case, no resonance phenomena appear when $A^{1/2}/B^{1/2}$ is exactly equal to $\frac{2}{3}$ (if the perturbation is not very large). Only for values of $A^{1/2}/B^{1/2}$ somewhat smaller than $\frac{2}{3}$ do we have resonant periodic orbits and tube orbits in general; if the perturbation is moderately large, we have to go rather far from the resonance to find the resonance phenomena.

Figure 1 gives the positions of the invariant points on the x-axis in the case $\epsilon = 0.1$

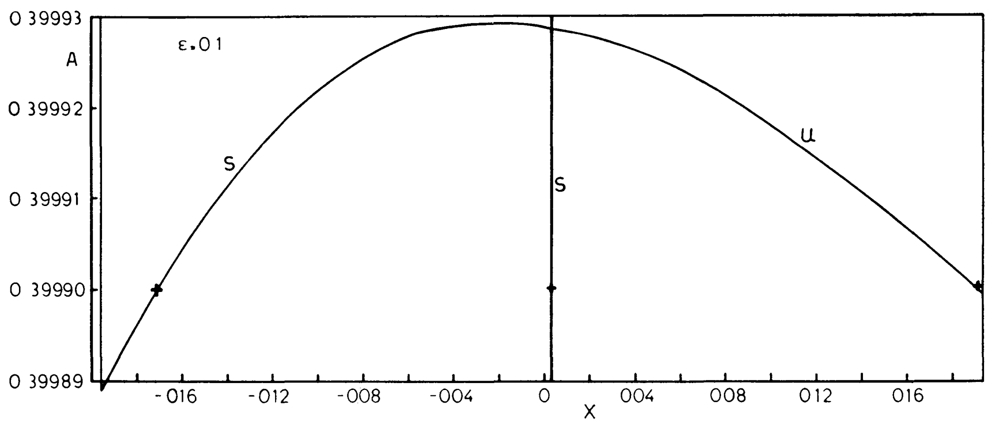

FIG. 1.—Positions of the invariant points on the x-axis, when $h = 0.00765$, $\epsilon = 0.1$, $B = 0.9$, and A is given on a vertical axis. S and U indicate stable and unstable invariant points. Crosses give the invariant points derived by means of the third integral. The limiting lines to the left and right are $x = \pm (2h/A)^{1/2} (\simeq \pm 0.194)$.

for various values of A, when $B = 0.9$, $h = 0.00765$. When $A > 0.39993$, there is no resonant periodic orbit making 2 and 3 oscillations along the x-axis and the y-axis, respectively. There is only one periodic orbit near the y-axis, perpendicularly intersecting the x-axis. The same is true when $A < 0.39989$. When $0.39993 > A > 0.39990$, there are three invariant points on the x-axis, the central one and two resonant invariant points, one stable (S, *left*) and one unstable (U, *right*). When A becomes smaller than 0.39990, the unstable invariant point to the right reaches the outer limit (the limiting curve $Ax^2 + X^2 = 2h$, in the plane x,X, which corresponds to the periodic orbit $y = 0$) and disappears. For $0.39990 > A > 0.39989$, we have only one (stable) resonant invariant point on the x-axis. When A becomes smaller than 0.39989, this point also reaches the limiting curve and disappears.

Using the third integral ϕ in the form (17), truncated after the terms of seventh degree, we find the positions of the invariant points as indicated by the crosses in the case $A = 0.39990$.

$$\text{Experiments—}0.171,\ 0.002,\ 0.189\ .$$

$$\text{Third integral—}0.171,\ 0.002,\ 0.190\ .$$

There is only a slight deviation in the case of the periodic orbit to the right.

The situation is similar when $\epsilon = 0.5$, except that for a range of values of A we have three resonant invariant points besides the central one. Figure 2 gives the positions of the invariant points (*solid line*) and the corresponding positions calculated by means of the third integral, truncated after the terms of seventh degree (*dashed line*).

The range of values of A for which we have at least one resonant invariant point besides the central one is from about 0.3984 down to about 0.3968. The letters S and U mean stable and unstable orbits, respectively (as found from their characteristic exponents).

The dashed curve shows the same behavior as the solid curve, although it does not agree completely with it. In one case ($A = 0.3981$), when terms up to the ninth degree were included in the third integral, the agreement between theoretical results (*crosses*) and experimental ones (*solid line*) was almost complete.

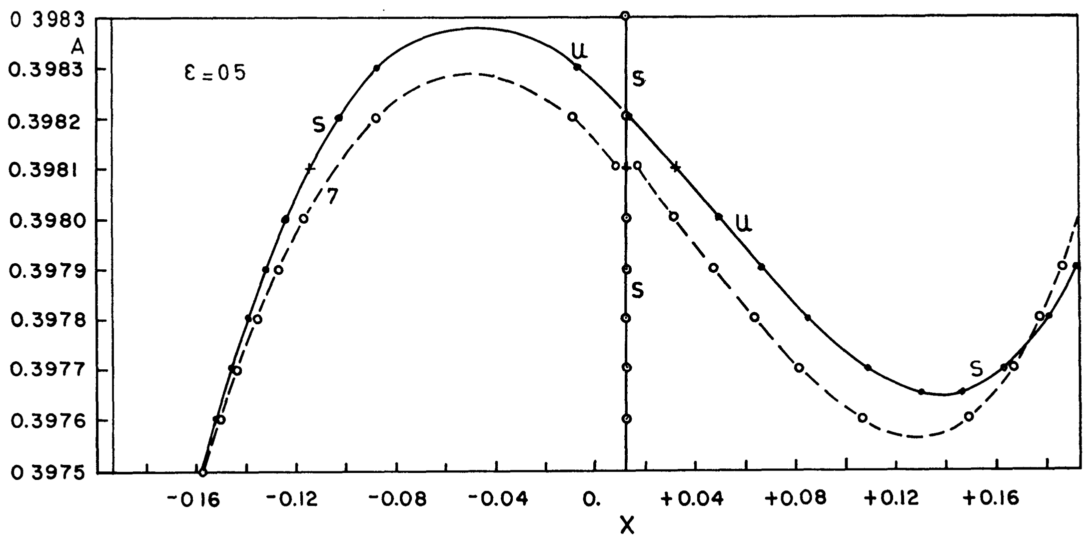

FIG. 2.—Same as in Fig. 1 for $h = 0.00765$, $\epsilon = 0.5$, $B = 0.9$. Solid line gives real positions of the invariant points, while dashed line gives invariant points derived by means of the third integral truncated after the seventh-order terms. Crosses give invariant points when the third integral is truncated after the ninth-order terms.

It is of interest at this point to show the positions of the invariant points calculated through the third integral truncated after the terms of the third, fourth, fifth, and sixth degree (Fig. 3).

If the third integral is truncated after the third-order terms (line marked *3*), only the central invariant point is found; the resonance phenomena are not apparent. If the third integral is truncated after the fourth-order terms (lines marked *4*), we eventually have two, or even three, invariant points, but rather far from the real ones, except for the left invariant point when $A = 0.3975$ (and, perhaps, for smaller values of A, also). When A becomes smaller or larger than the range shown in Figure 3, the two branches of line *4* tend, presumably, to line *3*, giving the central invariant point.

As the number of terms increases to five and six, the curves giving the invariant points approach more and more the real shape of the curve given by Figure 2, except for a range of values of A between approximately 0.3982 and 0.3977. This is due to the fact that in this range there are two roots relatively near each other and therefore the value of $\partial\bar{\Phi}/\partial\bar{x}$ never becomes very different from zero there (this has been checked directly); hence, any addition of higher-order terms may change considerably the roots of the equation $\partial\bar{\phi}/\partial\bar{x} = 0$. The same kind of deviation (but much smaller) is also seen in Figure 2 near the center for $A = 0.3981$.

The above results indicate the importance of using a sufficient number of terms of the third integral in applications in order to get sufficiently accurate results. The use of a non-convenient form of the third integral or of an insufficient number of terms may give quite wrong results.

The case $\epsilon = 1$ is similar to the case $\epsilon = 0.5$, but the range of values of A for which resonance phenomena appear (one, two, or three resonant invariant points, besides the regular [central] invariant point) is much larger, extending from $A = 0.395$ to $A \simeq 0.383$. The solid line in Figure 4 gives the real positions of the invariant points, while the dashed curve gives their positions derived by means of the third integral truncated after the terms of ninth degree. The agreement is rather good, except near $A = 0.393$, where the usual deviation is observed near the central invariant point. If we truncate the third integral before the terms of ninth degree, the agreement is worse, as in the case $\epsilon = 0.5$.

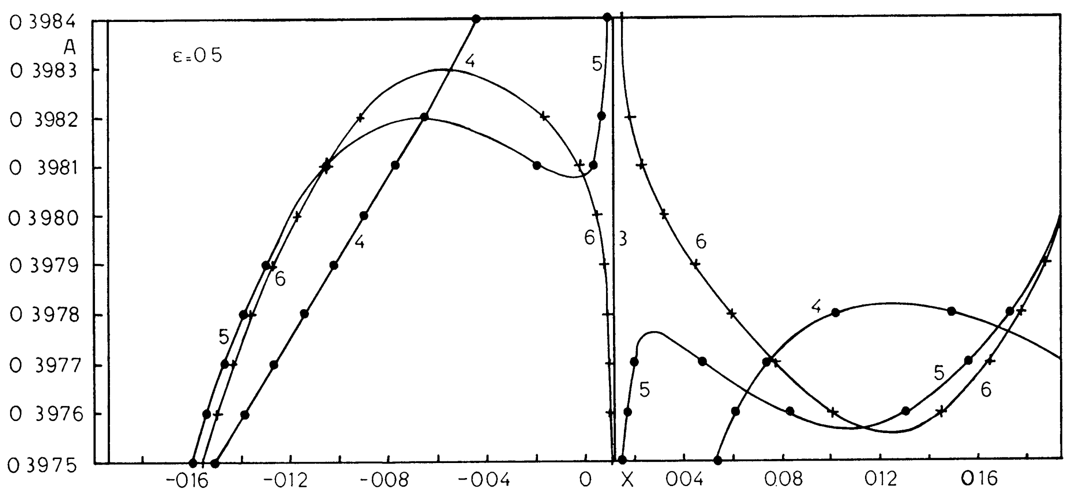

FIG. 3.—Expected positions of the invariant points when the third integral is truncated after the third-, fourth-, fifth, or sixth-order terms.

The limiting lines at the left and right in Figure 4 give the values of $x_{max/min} = \pm (2h/A)^{1/2}$; thus they are not parallel to the A-axis. The left branch of the curve extends down to $A \simeq 0.3825$ in this case.

Similar results are also found in the case $\epsilon = 2$ (Fig. 5). In this case, the range of values for which we have resonance phenomena extends from about $A = 0.405$ (even larger than 0.4) down to values of A even below the "escape" value $A \simeq 0.302$.

For $A < 0.302$, we have open curves of zero velocity, and the moving points may escape to infinity. This is because the curve of zero velocity $Ax^2 + By^2 - 2\epsilon xy^2 = 2h$ is open if y^2 becomes infinite for $x < x_{max} = (2h/A)^{1/2}$, i.e., for $A < 8h\epsilon^2/B^2 = 0.302. \ldots$

The invariant point at the left does not reach the outer boundary $-(2h/A)^{1/2}$ but reaches a minimum value $x \simeq -0.134$ for about $A = 0.325$, and for smaller values of A it moves to the right. This orbit is stable even beyond the "escape" value of $A \simeq 0.302$. It becomes unstable at about $A = 0.2995$. For smaller values of A it moves to the right, reaching the value $x = 0.094$ for $A = 0.20$. The "central" invariant point also moves to the right; it reaches the value $x = 0.343$ for $A = 0.12$. This orbit was found stable for all the values of A down to $A = 0.19$. Therefore, the stability of the periodic orbits does not depend directly on the "escape" value of A. A periodic orbit can be stable even when the curve of zero velocity is open.

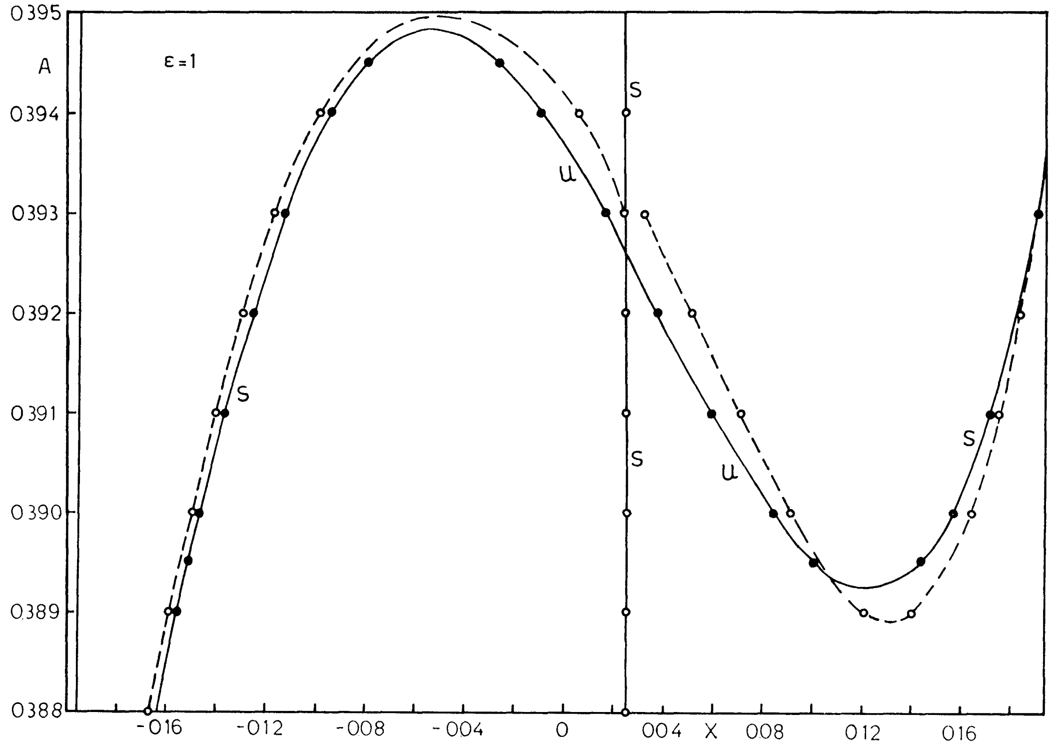

FIG. 4.—Same as in Fig. 1 for h = 0.00765, ϵ = 1, B = 0.9. Dashed line gives invariant points derived by means of the third integral truncated after the ninth-order terms.

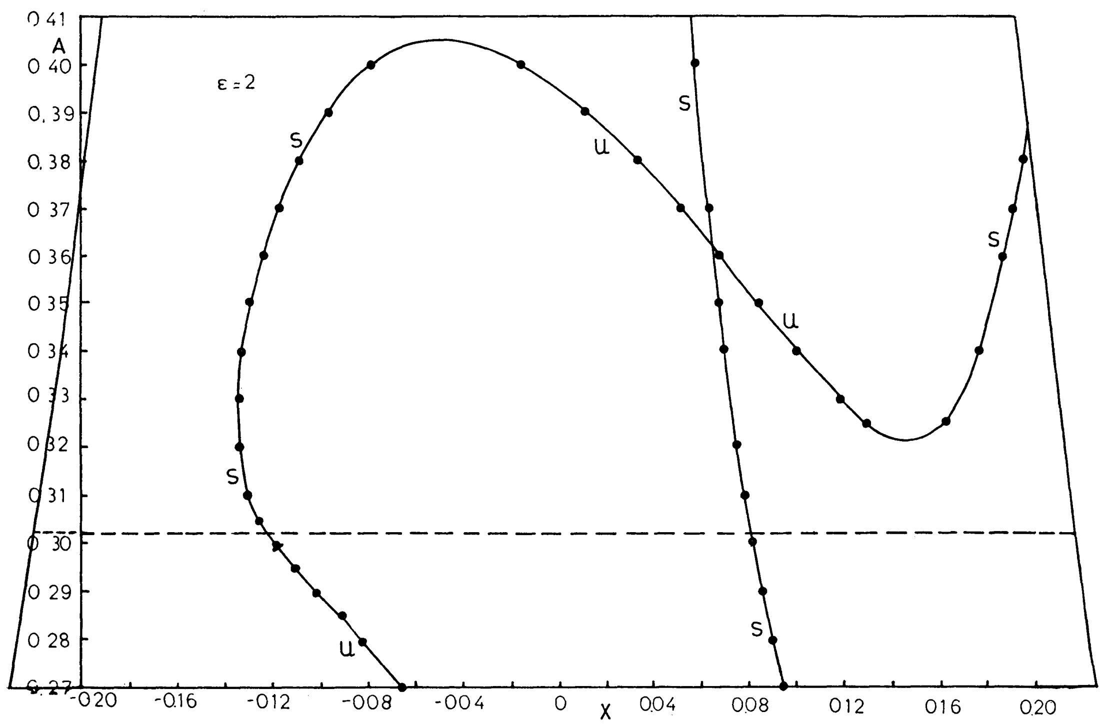

FIG. 5.—Same as in Fig. 1 for h = 0.00765, ϵ = 2, B = 0.9. Horizontal line represents the escape value of A. For smaller A, curves of zero velocity are open.

The relation between the invariant points and the other invariant curves is shown in Figures 6–9; these give the invariant curves for various values of A in the case $B = 0.9$, $\epsilon = 1$, $h = 0.00765$.

When $A = 0.394$ (Fig. 6), we have a set of regular invariant points near the central periodic orbit, on the right of the origin and near the limiting curve, which is a circle $\bar{x}^2 + X^2 = 2h$ in the plane $\bar{x},X$. We also have three sets of islands. Those to the left of the origin, on the $\bar{x}$-axis, center around the stable invariant point $\bar{x} = -0.058$, corresponding to the point $x = \bar{x}/A^{1/2} = -0.093$ of Figure 4. Near and to the left of the origin, there is an unstable invariant point. The invariant curve through it separates the islands from the inner and outer regular invariant curves. In Figure 6 this limiting invariant curve is drawn schematically as a dotted line. Its accurate calculation is very difficult; it requires too many calculations of orbits near the unstable periodic orbit. In

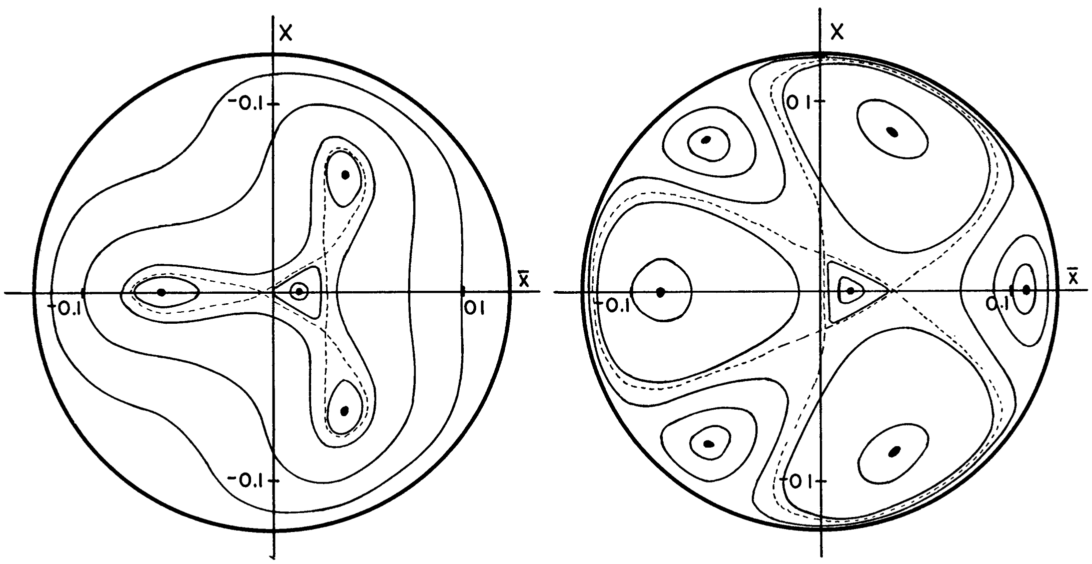

FIG. 6 (*left*).—Form of invariant curves on the surface of section $y = 0$ of the space $\bar{x}yX$, in the case $h = 0.00765$, $\epsilon = 1$, $B = 0.9$, $A = 0.394$. Outermost invariant curve is the circle $\bar{x}^2 + X^2 = 2h$, corresponding to the periodic orbit $y = 0$.

FIG. 7 (*right*).—Same as in Fig. 6 for $A = 0.391$.

reality, no invariant curve exists through the unstable invariant point; the intersections of orbits near the unstable periodic orbit by a surface of section show a small dispersion, i.e., they fill a strip of small but finite thickness (Contopoulos 1967). However, in the present case no such dispersion was discernible.

If A increases beyond 0.394, the stable and unstable invariant points to the left of the origin approach each other and disappear, together with the islands—e.g., for $A =$ 0.395 there are only regular invariant curves everywhere.

As A becomes smaller than about 0.3938, three new sets of islands appear near the outer limiting curve. One such set is to the right, near the $\bar{x}$-axis.

As A decreases, the unstable invariant point to the left of the origin moves to the right, and for $A \simeq 0.3926$ it coincides with the "central" invariant point. Then the "regular" invariant curves near the origin disappear. For still smaller A, e.g., for $A =$ 0.391 (Fig. 7), the unstable invariant point has moved to the right of the "central" invariant point and the set of "regular" invariant curves near the origin reappears. The invariant curve through the unstable invariant point is also drawn schematically in Figure 7. Outside it there are invariant curves of the regular type, i.e., invariant curves making one single loop around the central invariant point. Near the outer limiting curve, however, we have the new sets of islands, and the periodic orbit $y = 0$ is unstable.

As A decreases still further, the new sets of islands (right to the center near the $\bar{x}$-axis, etc.) approach nearer to the center, while the previous sets of islands (left to the center near the $\bar{x}$-axis, etc.) move outward (Fig. 8, $A = 0.3895$). For smaller A, the new set of invariant curves disappears, as the unstable invariant point to the right of the central invariant point, which moves outward as A decreases, coincides with the stable invariant point at the right, which moves inward. For even smaller A (Fig. 9, $A = 0.389$), only one set of islands near the outer limiting curve remains. As A decreases and reaches the value $A \simeq 0.3825$, these islands also disappear and only the regular invariant curves remain.

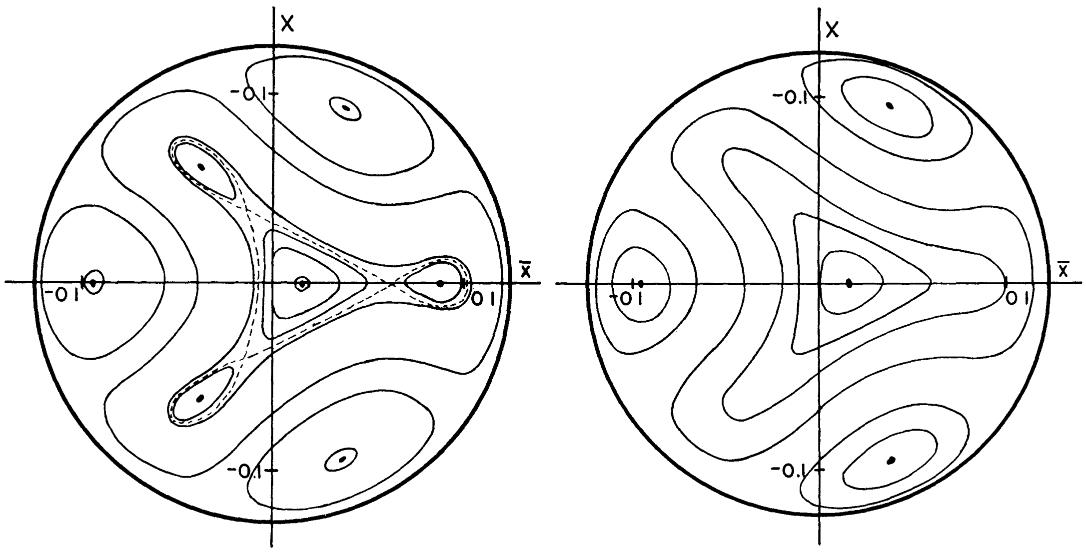

FIG. 8 (*left*).—Same as in Fig. 6 for $A = 0.3895$

FIG. 9 (*right*).—Same as in Fig. 6 for $A = 0.389$

From the above discussion it follows that the periodic orbit $y = 0$ is unstable whenever A is between approximately 0.3825 and 0.3938. This is verified by calculating the characteristic exponents of the periodic orbit $y = 0$.

Figure 10 gives the trace of the monodromy matrix (Wintner 1947). If the trace is between 0 and 4, the orbit is stable. In the present case, it is seen that for a range of values of A between 0.3825 and 0.3938 the trace is negative; therefore, the orbit $y = 0$ is unstable. This was expected because the orbits near $y = 0$, for this range of values of A, do not give simple invariant curves near the outer limiting curve, but give also branches extending inward (Figs. 7–9).

V. CONCLUSIONS

It is evident that the main characteristics of the invariant curves can be easily predicted if we know the positions of the invariant points. It is even sufficient to know the invariant points on the $\bar{x}$-axis because then the other invariant points can be easily located approximately.

The stable invariant points are the centers of sets of islands, which correspond to tube orbits. The unstable invariant points are also important, first, because they separate the invariant curves of different types (Figs. 6–9) and, second, because any "dissolution" of the invariant curves is apparent near the unstable periodic orbits.

Therefore, instead of calculating many invariant curves, which is a tedious and time-consuming procedure, one can calculate the main invariant points, corresponding to the regular and resonant periodic orbits; then the calculation of one or two non-periodic orbits near the unstable periodic orbits gives the degree of "dissolution" of the invariant curves.

The initial conditions of the periodic orbits and their stability behavior can be found by using the correct form of the third integral in each case.

The above considerations can be applied to models of the Galaxy, in order to give the main types of orbits for a set of values of the energy, without detailed calculations. The theoretical approach by means of the third integral can be applied if the potential is given as a polynomial in the variables.

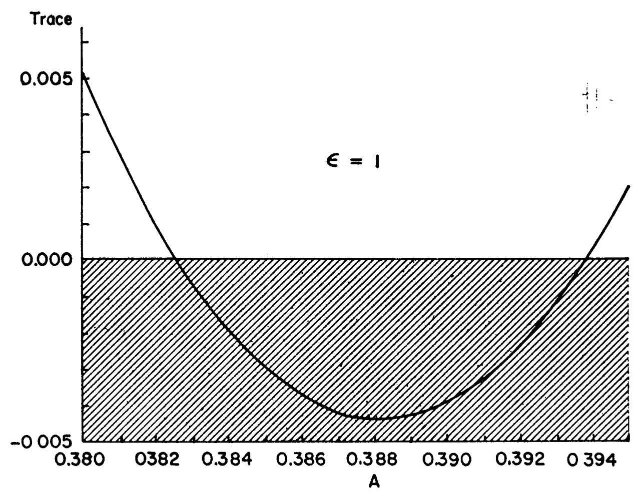

FIG. 10.—Trace of the monodromy matrix in the case $h = 0.00765$, $\epsilon = 1$, $B = 0.9$, for various values of A. Shaded area indicates instability.

Part of this work was done while I was a senior research associate of the National Research Council–National Academy of Sciences at the Institute for Space Studies, New York. The extensive numerical calculations were made with the help of the IBM 350-75 computer of the Institute for Space Studies and the IBM 1620 computer of the University of Thessaloniki. I thank Dr. J. Hadjidemetriou for much help in the numerical calculations.

REFERENCES

Contopoulos, G. 1960, *Zs. f. Ap.*, **49**, 273.
———. 1965, *A.J.*, **70**, 526.
———. 1966, *Ap. J. Suppl.*, **13**, 122.
———. 1967, *B.A.*, **2**, No. 1, 223.
Wintner, A. 1947, *The Analytical Foundation of Celestial Mechanics* (Princeton, N.J.: Princeton University Press), p. 104.